Controlled Dephasing of a Quantum Dot: From Coherent to Sequential Tunneling

Daniel Rohrlich,* Oren Zarchin,† Moty Heiblum, Diana Mahalu, and Vladimir Umansky

Braun Center for Submicron Research, Department of Condensed Matter Physics, Weizmann Institute of Science, 76100 Rehovot, Israel

(Received 17 July 2006; published 1 March 2007)

Resonant tunneling through two identical potential barriers renders them transparent, as particle trajectories interfere coherently. Here we realize resonant tunneling in a quantum dot (QD), and show that detection of electron trajectories renders the dot nearly insulating. Measurements were made in the integer quantum Hall regime, with the tunneling electrons in an inner edge channel coupled to detector electrons in a neighboring outer channel, which was partitioned. Quantitative analysis indicates that just a few detector electrons completely dephase the QD.

DOI: 10.1103/PhysRevLett.98.096803 PACS numbers: 73.23.Hk, 03.65.Ta, 03.65.Yz

The study of entanglement began in 1935 with the EPR and Schrödinger Cat paradoxes, but it languished until Bell's celebrated theorem and even thereafter. More recently, applications of entanglement to cryptography, "teleportation," data compression, and computation [1] have given new impetus to the study of entanglement. Also "dephasing" ("decoherence") is studied, both as a condition for classical behavior to emerge and as an obstacle to applications of entanglement. Here we report controlled partial and full dephasing of electron interference in a mesoscopic Fabry-Perot type of interferometer—a quantum dot (QD)—entangled efficiently to a mesoscopic detector.

Mesoscopic interferometers [2] include closed and open two-path interferometers, QDs and double-QDs, and electronic Mach-Zehnder interferometers. Mesoscopic detectors [2] include quantum point contacts (QPCs) and partitioned currents. In our experiment, a QD serves as an interferometer of the Fabry-Perot type; the interference shows up as a resonant transmission peak in electron conductance through the dot. Figure 1 shows the device, including the QD. The dark gray strips represent charged gates. Rectangles along the edge of the device represent Ohmic contacts; tunneling electrons enter the device at the Ohmic contact marked V_S. We worked at filling factors $\nu = 2$ and $\nu = 3$ in the integer quantum Hall effect regime, but nothing in our results depends essentially on edge channels or a magnetic field. In Fig. 1 we have $\nu = 2$, so electrons enter in two edge channels. The magnetic field turns electrons to their right but the gates repel them. As electrons from V_S arrive at QPC 1, those in the outer quantum Hall edge channel (closest to the gates) make a right turn through QPC 1, while those in the innermost channel reflect towards the QD. Thus all electrons tunneling through the QD come from the inner edge channel. For these electrons, the dot is an interferometer. (In general, electrons can "relax" from one channel to the other; such relaxation is measurable at QPC 4. We chose settings to eliminate relaxation.)

To couple tunneling and "detector" electrons strongly, we chose them from neighboring edge channels, in close proximity. As electrons in the inner edge channel tunnel through the dot, they become entangled with electrons passing freely through the neighboring, outer (detector) edge channel. The source of these detector electrons is the Ohmic contact marked V_D, and only electrons in the outer edge channel pass through QPC 1 on their way to the QD. These detector electrons couple Coulombically to the total charge Q_{tun} tunneling through the dot, and their accumulated phase is proportional (via this Coulomb coupling) to the dwell time t_{dwell} of the tunneling electrons: $Q_{\text{tun}} = t_{\text{dwell}} I_{\text{tun}}$, where I_{tun} is the tunneling current.

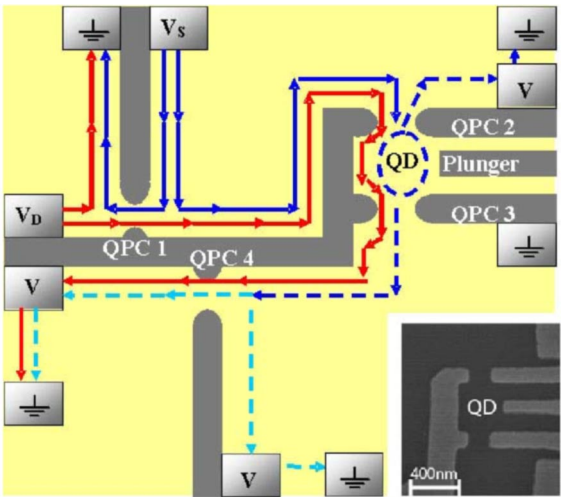

FIG. 1 (color online). Diagram of the device: the dot (not to scale) comprises QPC 2, a "plunger gate" and QPC 3. Tunneling electrons reflect from QPC 1 to the dot; detector electrons pass through QPC 1 to the dot. (Edge channels at zero potential are not shown.) In practice, an additional negative potential is applied to QPC 1 to partition the outer (detector) edge channel, so all of the inner and part of the outer edge channels are reflected at QPC 1. Inset: SEM micrograph of a similar dot, 0.4 μm wide inside.

Detection broadens and quenches the resonance, consistent with the time-energy uncertainty principle: decreased uncertainty in the dwell time entails increased uncertainty in the energy of the electrons.

According to a general principle [3], any determination of the path an electron takes through an interferometer, among all possible interfering paths, destroys the interference among the paths. Hence, coupling (entangling) a trajectory-sensitive detector and an electron interferometer should destroy the interference. In our experiment the detector is the partitioned outer channel current; it is partitioned at QPC 1 before reaching the QD. Why partitioned? Electrons in the outer (detector) edge current acquire a phase due to Coulomb coupling with the tunneling electrons in the innermost channel. However, if the outer edge current is full (unpartitioned, noiseless) as in Fig. 1, this phase is in principle unobservable. (As for interference between the two edge channels—they cannot interfere, because they never overlap.) Partitioning the detector current produces a transmitted and a reflected outer edge current; these two currents could interfere elsewhere and render the unobservable phase observable. Thus partitioning the detector current allows us to extract the additional phase due to coupling with electrons tunneling through the quantum dot. Now, whether or not we actually interfere the transmitted and reflected currents elsewhere cannot instantly produce any measurable change at the dot. Hence, the partitioned outer edge current must by itself dephase the electron resonance in the interferometer.

In this account, dephasing arises because the interfering quanta (tunneling electrons) leave ''which path'' information in the environment (detector current). But another general principle [4] offers a complementary account: dephasing arises because the environment (partitioned detector current) produces a fluctuating phase in the interfering quanta. If N electrons in the outer edge channel arrive at QPC 1 and pass through with probability T, then NT are transmitted, on average, with typical fluctuations of order $\sqrt{NT(1-T)}$. These fluctuations in the detector current (''shot noise'' [5]) produce a fluctuating potential at the dot and thus a fluctuating phase in the tunneling electrons, which dephases the resonance.

For a Fabry-Perot interferometer, we can model the dephasing by calculating the effect of detection on interference. Let QPC 2 and QPC 3 of the dot (in Fig. 1) transmit with amplitudes t_2 and t_3 and reflect with amplitudes r_2 and r_3, respectively. The amplitude t_{tun} for resonant transmission through the dot is

$$t_{\mathrm{tun}} = t_2 t_3 \sum_{j=0}^{\infty} (r_2 r_3)^j e^{i(2j+1)\theta} e^{i\Phi_j} \qquad (1)$$

and includes an energy-dependent phase 2θ for each back-and-forth lap in the interferometer. We assume that during each lap, N detector electrons reach QPC 1 (which partitions the detector current). Each transmitted detector electron contributes an additional phase ϵ to the back-and-forth lap of the resonant-tunneling electron, while reflected detector electrons contribute no phase. Indexing the detector electrons $k = 0, 1, 2, \ldots$ according to their order of arrival at QPC 1, we have additional phases ϵ_k where $\epsilon_k = \epsilon$ if the kth electron is transmitted through QPC 1 and $\epsilon_k = 0$ if it is reflected. Then, for a given partitioning of the detector current, we have $\Phi_j = \sum_{k=1}^{jN} \epsilon_k$. (Actually, t_{tun} contains also an overall phase due to the first $N/2$ detector electrons to reach QPC 1—as the tunneling electron first crosses the interferometer—common to all the terms in the sum.) The transmission probability, given this partitioning, is the square of the absolute value of Eq. (1):

$$T_{\mathrm{tun}} = T_2 T_3 \sum_{j,j'=0}^{\infty} (r_2 r_3)^j (r_2^* r_3^*)^{j'} e^{2(j-j')i\theta} e^{i\Phi_j - i\Phi_{j'}}, \qquad (2)$$

where $T_2 = |t_2|^2$, etc. We have to fold Eq. (2) with the probability distribution for the partitioning of detector electrons. Each ϵ_k is independently distributed; with probability R, the kth electron is reflected from QPC 1, in which case $e^{i\epsilon_k} = 1$, and with probability T it is transmitted, in which case $e^{i\epsilon_k} = e^{i\epsilon}$. Thus the expectation value of $e^{i\epsilon_k}$ is $R + e^{i\epsilon}T$ and the expectation of $e^{i\Phi_j - i\Phi_{j'}}$ is $(R + e^{i\epsilon}T)^{(j-j')N}$. Next we fix $j - j' \geq 0$, sum over j', and finally sum over all $j - j'$. (The sum over $j - j' < 0$ is the complex conjugate of the sum over $j - j' > 0$.) Now the transmission probability, which we denote $\langle T_{\mathrm{tun}} \rangle$ to indicate the averaging over detector partitionings, is

$$\langle T_{\mathrm{tun}} \rangle = \frac{T_2 T_3}{1 - R_2 R_3} \left[\frac{1}{1 - M} + \frac{1}{1 - M^*} - 1 \right], \qquad (3)$$

where $M \equiv e^{2i\theta} r_2 r_3 (R + e^{i\epsilon}T)^N$. The integral of $\langle T_{\mathrm{tun}} \rangle$ over $\bar{\theta} \leq \theta \leq (\bar{\theta} + \pi)$, for any real $\bar{\theta}$, is independent of $|M|$ (as it must be since probabilities must sum to 1 whatever the dephasing). For $R_{2,3} \gg T_{2,3}$ and small ϵ, Eq. (3) implies both broadening and quenching (decreased height) of the resonance peak in proportion to $NT(1-T)$, as derived before [6]. Here, however, with the detector and tunneling currents so close, we cannot assume ϵ small.

The device, constructed from a GaAs-AlGaAs heterojunction, supported a high-mobility two-dimensional electron gas (2DEG) of density $3 \times 10^{11}/\mathrm{cm}^2$. Biased metallic gates deposited on the surface of the heterojunction induced a controlled backscattering potential to form the QD and QPCs. The magnetic field was 5–7 T, well within the filling-factor 2 conductance plateau. Conductance was measured with a 0.9 MHz AC, 0.5 μV RMS excitation voltage at an electron temperature of $\tau = 25$ mK (determined by measurements of thermal noise and shot noise as in Ref. [7]). A low-noise cryogenic preamplifier near the sample amplified the measured voltage, followed by a room-temperature amplifier and a spectrum analyzer. An LC resonant circuit prior to the cold preamplifier determined the bandwidth of about 100 Hz around 0.9 MHz; see Refs. [7,8] for details.

Figure 2 shows dephasing of a series of Coulomb blockade peaks for various partitionings T of the detector current, at detector bias $V_D = 77\ \mu$V. For the horizontal axes we convert plunger gate potential to an effective dot potential (a "levering factor" extracted from Coulomb-diamond measurements [9]). The resonance peaks quench and broaden as T increases from 0 to $\frac{1}{2}$ and reemerge as T increases from $\frac{1}{2}$ to 1. At $T = 0$ there is no current in the detector to dephase the resonance. At $T = 1$ the resonance induces a constant—but unobservable—phase in the electrons of the detector current, and there is again no dephasing. Only at intermediate T does the detector current contain information about the resonance, and dephase it. Smaller detector bias implies less information (or, in the complementary account, less shot noise) in the detector current, hence less dephasing. Indeed, resonance peaks are less quenched at smaller detector bias.

Looking in detail at one conductance peak and fitting it with a Lorentzian curve, we obtain the width of the resonance peaks, as in Fig. 2(b). Undephased peaks have a full width at half maximum (FWHM) of about 12 μV, larger than $4k_B\tau \approx 9\ \mu$V (where k_B denotes the Boltzmann constant). We found that T depended slightly on the detector bias. Thus, for each value of detector bias, we calculated an effective transmission $T_{\rm eff}$ by averaging T with respect to energy, from the Fermi energy to the detector bias, and Fig. 3 shows dependence of (a) peak height and (b) peak width on $T_{\rm eff}$, with the bias on the detector as an additional parameter.

For a quantitative relation between shot noise and dephasing, let us define 3 times: $t_{\rm dwell}$, $t_{\rm lap}$, and $t_{\rm det}$. In the absence of temperature broadening, the dwell time $t_{\rm dwell}$ would be $\hbar$ divided by 12 μV, the FWHM of the resonance. However, the FWHM is a convolution of coherent broadening and temperature broadening; only the former is relevant to the dwell time. Subtracting the temperature

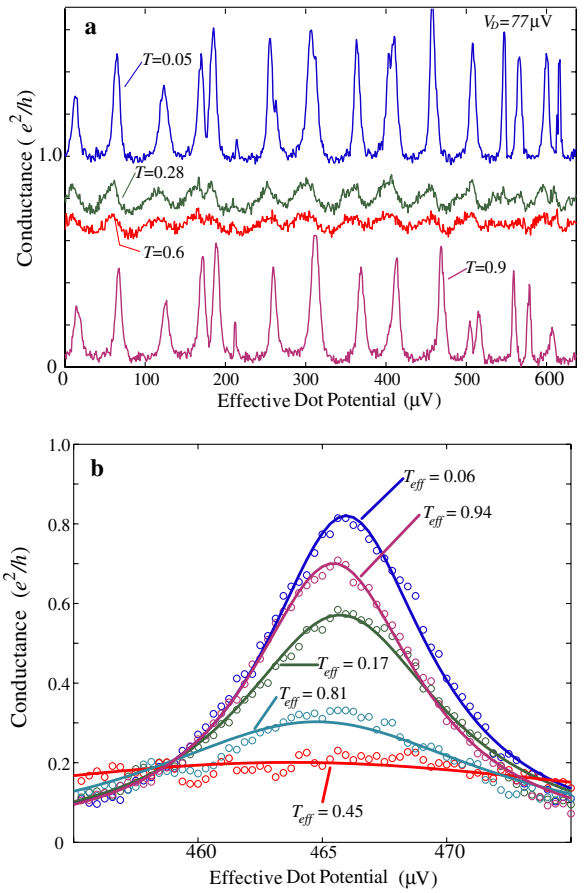

FIG. 2 (color online). Dephasing of resonance peaks at filling factor 2, with 77 μV detector bias. (a) The horizontal axis shows the potential on the plunger gate, normalized to effective dot potential. The vertical axis shows the resonant conductance through the inner channel (shifted for clarity), from $T \approx 0$ to $T \approx 1$. (b) Dephasing of a typical resonance peak. Circles are experimental results while lines are Lorentzian fits.

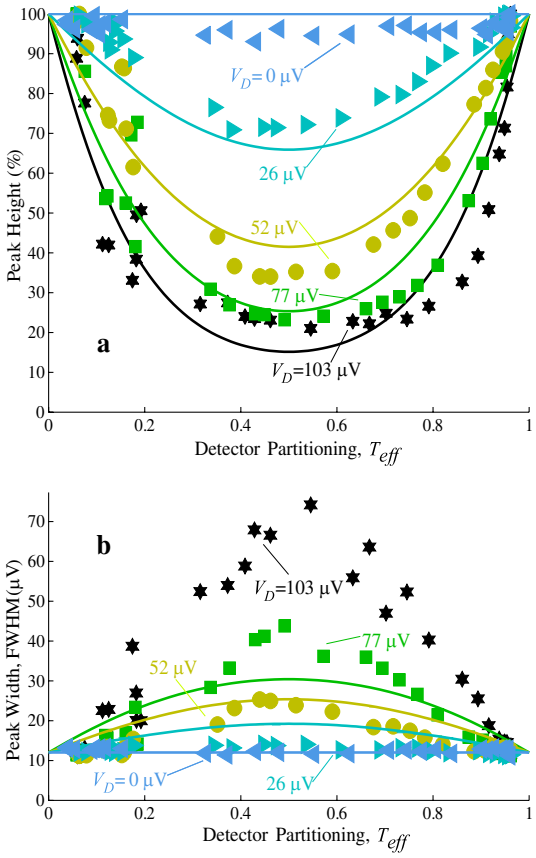

FIG. 3 (color online). Plots of (a) quenching (as percentage of the original peak height) and (b) peak width FWHM, as functions of $T_{\rm eff}$ and detector bias. Symbols denote experimental results. In (a), curves are fits to Eq. (4) with $\epsilon = \pi/2$; $N = 4$ for maximum detector bias $\pm 103\ \mu$V. We can estimate ϵ by biasing the unpartitioned detector channel; the resulting shifts in the resonance peaks suggest that each transmitted detector electron increases the energy of the tunneling electron by some 4 μeV. Then $\epsilon \approx (4\ \mu\text{eV})(t_{\rm lap})/\hbar$ is of order 1, consistent with $\epsilon = \pi/2$ and with strong dephasing due to a few detector electrons. In (b), curves are fits to Eq. (5) with the same N, ϵ and detector biases.

broadening $4k_B\tau \approx 9\ \mu$V from 12 μV we are left with 3 μV, so $t_{\rm dwell} \approx \hbar/3\ \mu{\rm V} \approx 220$ psec.

The dwell time is a multiple of the lap time, i.e., the time $t_{\rm lap}$ it takes an electron to go once back-and-forth in the dot. How many laps in a dwell time? To answer this question we return to Eq. (1) and note that the jth term in the series corresponds to $j + \frac{1}{2}$ laps. Then the average number of laps of a tunneling electron is $\sum_j (j + 1/2) T_2 T_3 (R_2 R_3)^j$ divided by the total probability $\sum_j T_2 T_3 (R_2 R_3)^j$ to tunnel through the resonance, i.e., it is $\frac{1}{2} + R_2 R_3/(1 - R_2 R_3)$. In our QD we estimate $R_2 \approx R_3 \approx \frac{2}{3}$ and so the average number of laps was approximately 1.3. Dividing $t_{\rm dwell}$ by 1.3, we obtain $t_{\rm lap} \approx 170$ psec as the lap time. (From $t_{\rm lap}$ we can estimate the speed of an electron tunneling through the dot: if the effective inner length of the dot was roughly 0.25 μm, then the electron traveled 0.5 μm in 170 psec, i.e., its speed was roughly 3×10^5 cm/sec, corresponding to a rather small electric field in the dot.)

Finally, the time $t_{\rm det}$ between successive electrons in the unpartitioned detector current I is $e/I = eR_H/V_D$ where $R_H = h/e^2$ is the Hall resistance and V_D is the bias applied to the detector. Thus, $t_{\rm det} = h/eV_D$, which was as low as 40 psec for the maximum detector bias of 103 μV. For this bias, an average of 170 psec/40 psec ≈ 4 detector electrons reached QPC 1 during each lap of the tunneling electron, and proportionally fewer for smaller bias. This number corresponds to N.

Taking N proportional to the detector bias potential V_D, we find experimentally that broadening and quenching of the resonance peak are both proportional to the shot noise $NT_{\rm eff}(1 - T_{\rm eff})$ at low bias ($10\ \mu{\rm V} \le V_D \le 50\ \mu$V) but deviate from simple proportionality at larger bias. Figure 3(a) shows that at larger bias, quenching of the resonance peak tends to saturate before $T_{\rm eff}$ reaches 0.5. This saturation is just what Eq. (3) implies, since the peak height (i.e., the maximum value of $\langle T_{\rm tun}\rangle$ as a function of θ) obtained from Eq. (3) is

$$\text{peak height} = \frac{T_2 T_3}{1 - R_2 R_3} \frac{1 + \sqrt{Z}}{1 - \sqrt{Z}}, \tag{4}$$

where $Z \equiv R_2 R_3 [1 + 2RT(\cos\epsilon - 1)]^N$. Equation (4) depends linearly on the shot noise $NRT = NT(1 - T)$ for small ϵ, but when ϵ is not small, Eq. (4) saturates in T for large bias (large N), as the fits to Fig. 3(a) show.

Equation (3) leads also to a formula for peak broadening as a function of detector bias and partitioning:

$$\text{FWHM} = \frac{\hbar}{t_{\rm lap}} \arctan\frac{1}{2}\left[\frac{1}{\sqrt{Z}} - \sqrt{Z}\right]. \tag{5}$$

Equation (5) implies saturation of broadening before $T_{\rm eff}(1 - T_{\rm eff})$ reaches its maximum value, for large bias. Yet Fig. 3(b) indicates "antisaturation" in $T_{\rm eff}$: that is, the data do not level off in the middle of the range of $T_{\rm eff}$ but cluster upwards in the form of a triangle. This apparent inconsistency with our model is an artifact of the multiplicity of peaks. Each peak is enhanced by the tails of its neighbors, and this enhancement increases as the peaks dephase. It hardly affects the height of a peak, which is measured farthest from the neighboring peaks, but strongly affects broadening. Hence we have not applied Eq. (5) to Fig. 3(b) for the largest bias.

Additional support for our analysis of dephasing comes from our measurements on the same mesoscopic device, but with another setup, at filling factor 3 and electron temperature of $\sim$100 mK. In these measurements, electrons in the partitioned middle edge channel "detected" tunneling electrons in the innermost edge channel, at magnetic fields 4.0 and 4.3 T. Since these edge channels are separated by a cyclotron gap, we expect a larger channel separation, hence weaker dephasing (smaller ϵ). For small ϵ, Eqs. (3) and (5) imply a broadening in FWHM proportional to $NRT\epsilon^2$. Indeed, we found that the FWHM depended linearly on $IT_{\rm eff}(1 - T_{\rm eff})$ and that the slope of this linear dependence was 40% higher at 4.0 T than at 4.3 T, i.e., dephasing was stronger at smaller channel separation.

In summary, we have demonstrated controlled dephasing of a resonant-tunneling device (a quantum dot) and showed how the dephasing depends on the detector current and partitioning. We exploited the close proximity of edge channels in the integer quantum Hall regime to strongly entangle a small number of electrons.

We thank Yang Ji, Yunchul Chung, Michal Avinun, and Izhar Neder for technical help and Florian Marquardt and Izhar Neder for helpful discussions. This work was partly supported by the MINERVA Foundation, the German Israeli Foundation (GIF), the German Israeli project cooperation (DIP), the Israeli Science Foundation (ISF), and by the Israeli Ministry of Science and Technology.

*Present address: Department of Physics, Ben-Gurion University, 84105 Beersheva, Israel.
†Email address: oren.zarchin@weizmann.ac.il

[1] See *Introduction to Quantum Computation and Information*, edited by H.-K. Lo, S. Popescu, and T. P. Spiller (World Scientific, Singapore, 1998).
[2] For a review, see D. Rohrlich, Opt. Spectrosc. **99**, 503 (2005).
[3] R. P. Feynman, R. B. Leighton, and M. Sands, *The Feynman Lectures on Physics* (Addison-Wesley Pub. Co., Reading, MA, 1965), Vol. III, pp. 1–9.
[4] A. Stern, Y. Aharonov, and Y. Imry, Phys. Rev. A **41**, 3436 (1990).
[5] For a review, see M. Reznikov *et al.*, Superlattices Microstruct. **23**, 901 (1998). The term "shot noise" is often identified with the factor $NT(1 - T)$.
[6] J. H. Davies, J. C. Egues, and J. W. Wilkins, Phys. Rev. B **52**, 11 259 (1995). For ϵ small, we have $|R + e^{i\epsilon}T|^N \approx e^{-NRT\epsilon^2/2} = e^{-NT(1-T)\epsilon^2/2}$.
[7] R. de-Picciotto *et al.*, Nature (London) **389**, 162 (1997).
[8] M. Reznikov *et al.*, Nature (London) **399**, 238 (1999).
[9] L. P. Kouwenhoven, D. G. Austing, and S. Tarucha, Rep. Prog. Phys. **64**, 701 (2001).